

# Long-term climate simulation in NorESM: burst-coupling the sediment in the BLOM/iHAMOCC ocean module

Marco van Hulten<sup>1,3</sup>, Christoph Heinze<sup>1,2,3</sup>, Jörg Schwinger<sup>2,3</sup>, and Jerry Tjiputra<sup>2,3</sup>

<sup>1</sup>Geophysical Institute, University of Bergen, Allégaten 70, 5007 Bergen, Norway

<sup>2</sup>NORCE Norwegian Research Centre AS, 5838 Bergen, Norway

<sup>3</sup>Bjerknes Centre for Climate Research, Norway

**Correspondence:** M. M. P. van Hulten <marco@hulten.org>

**Abstract.** In this report we set forth a simulation method for long-term simulations of NorESM, the Norwegian Earth System Model. In this the sediment is repeatedly decoupled and coupled to the ocean model (BLOM/iHAMOCC), a process called *burst coupling*. Through this, the ocean (seawater and sediment) is brought into an approximate steady state. We show that just the model has to run at least 50 000 yr to get in an approximate steady state. With burst coupling this can be done in a computationally reasonable time (wall time in the order of one week). The method can be used to generate the sediment over hundreds of thousands of years, so it is useful not only for present-day simulations but also for paleo-climatological studies.

## 1 Introduction

The ocean plays a major role in the regulation of the past and present climate. It has the capacity to absorb huge amounts of heat, as illustrated by the fact that the ocean was the dominating net heat sink in the Earth system during 1971–2018 (IPCC, 2021). The ocean is also a big net carbon sink (Sabine et al., 2004; Steinfeldt et al., 2009). The preservation of carbon, both in its organic and inorganic form, affects the long-term climate (Archer and Maier-Reimer, 1994, for calcite). These effects are long-term, but we need to consider them even for the present climate. When we model the present climate, the full physical and biogeochemical system from upper ocean (fast) down into the sediment (slow) needs to approximate a steady state. This can be achieved through model simulation of the ocean (either coupled to the atmosphere or stand-alone). The ocean circulation is operating at a time scale of hundreds to thousands of years. Reaching an approximate steady state of the physical and biogeochemical

system (complete mixing of the ocean) takes more time. The sediment is even slower and takes at least tens of thousands of years to converge to a steady state. However, using direct model integration, the simulation of the water column is computationally slower and much more expensive than that of the sediment. In any case, it is not feasible to do a coupled integration of an ocean model for tens of thousands of years.

There are several reasons why we are studying the sediment in the light of understanding and prognosis of the climate. Firstly, sediment traces climate variations in the past. Secondly, the sediment is a constraint on the particle fluxes simulated (the sediment is the best sediment trap). Thirdly, fluxes between the sediment and the water column are important (oxygen, alkalinity, carbon, silicic acid and other nutrients). The  $\text{CaCO}_3$  dissolution feedback is important for fossil fuel  $\text{CO}_2$  neutralisation.

A pilot study on the use of sediment observations combined with a modelling approach (forward and inverse) was published by Heinze et al. (2016) using the simpler, annually averaged HAMOCC2 model. The model allows for artificial sediment core development in order to directly compare model data with sediment core measurements. In the pilot study, the modelling approach was successful in attributing a series of processes as likely candidates for causing the 80–100 ppm reduction of atmospheric  $\text{CO}_2$  at the last ice age.

Whereas those simulations were very useful to get insight in the first-order effects of the processes related to climatic changes at the end of the last ice age, a state-of-the-art biogeochemical model simulation is useful for a more realistic analysis. In this report we set forth a simulation method for long-term simulations of NorESM, the Norwegian Earth System Model. In this the sediment is repeatedly decoupled from and coupled to the ocean model (BLOM/iHAMOCC), a process hereafter called *burst coupling* (Hasselmann, 1991). Through this, the ocean (seawater and sediment) is brought into an approximate steady state. We will show how long the

system has to run to get in a steady state. We will show how fast the burst coupling method is; if a long simulation can be done in a computationally reasonable time.

## 2 Methods

### 2.1 Model description

We use the isopycnic general circulation model BLOM (Bergen Layered Ocean Model), which was originally developed from the Miami Isopycnic Coordinate Ocean Model (MICOM) (Bentsen et al., 2013). We use the model within the framework of the Norwegian Earth System Model (NorESM) (Kirkevåg et al., 2013), but in this study the ocean is the only active (online) component. Hence this section describes only the ocean model; the other parts of the Earth system (atmosphere, land and sea ice) do not run on-line in this study but are data components that force the ocean.

#### 2.1.1 Seawater processes

The biogeochemistry is part of BLOM and is referred to as the isopycnic HAMburg Ocean Carbon Cycle (iHAMOCC). It is a NPZD-type (nutrients–phytoplankton–zooplankton–detritus) model extended to include Dissolved Organic Carbon (DOC). The model iHAMOCC simulates the cycles of carbon, three major nutrients (phosphate, nitrate and silica) and the trace nutrient iron, along with phytoplankton, a zooplankton grazer, detritus or henceforth Particulate Organic Carbon (POC), as well as calcium carbonate ( $\text{CaCO}_3$ ) and biogenic silica ( $\text{bSiO}_2$ ). A constant Redfield ratio of  $\text{P} : \text{C} : \text{N} : \text{O}_2 = 1 : 122 : 16 : -172$  is used (Takahashi et al., 1985). Further details on the ecosystem model can be found in Maier-Reimer et al. (2005); Schwinger et al. (2016). We continue with a description of what is most relevant for the sediment, namely the particles in the seawater.

Lithogenic clay is added into the top layer of the ocean, as a refractory tracer of unknown composition (assuming quartz for its density) as well as a direct input of iron through the instant dissolution of the deposited dust. Besides dust input, there is river input of dissolved components into the ocean, as well as of POC (Tjiputra et al., 2020). We use a parameterisation for organic carbon particles that linearly increase their sinking speed with depth to account, in a crude way, for aggregation. The other particles, clay,  $\text{CaCO}_3$  and  $\text{bSiO}_2$ , sink through the water column with a homogeneous velocity. There is only one size class of each of the particles and each has a unific reactivity. The remineralisation rates for POC and  $\text{bSiO}_2$  are constant, whereas the dissolution of  $\text{CaCO}_3$  depends on its saturation state (using first-order dissolution kinetics).

#### 2.1.2 Sediment processes

The model’s sediment module contains four solid compounds and seven solutes (Table 1). Each of these tracers has a counterpart in the seawater.

symbol	meaning	units
<i>state variables of the solid fraction (s)</i>		
OC	organic carbon	$\text{mol}_\text{P} \text{ dm}^{-3}$
$\text{CaCO}_3$	calcium carbonate	$\text{mol}_\text{C} \text{ dm}^{-3}$
$\text{bSiO}_2$	biogenic silica	$\text{mol}_\text{Si} \text{ dm}^{-3}$
clay	lithogenic (from dust)	$\text{kg m}^{-3}$
<i>state variables of the porewater solutes (d)</i>		
DIC	dissolved inorganic carbon	$\text{mol}_\text{C} \text{ dm}^{-3}$
$A_T$	total alkalinity	$\text{equiv dm}^{-3}$
$\text{PO}_4$	phosphate	$\text{mol}_\text{P} \text{ dm}^{-3}$
$\text{O}_2$	oxygen	$\text{mol}_\text{O}_2 \text{ dm}^{-3}$
$\text{N}_2$	molecular nitrogen	$\text{mol}_\text{N} \text{ dm}^{-3}$
$\text{NO}_3$	nitrate	$\text{mol}_\text{N} \text{ dm}^{-3}$
$\text{Si(OH)}_4$	silicic acid	$\text{mol}_\text{Si} \text{ dm}^{-3}$

**Table 1.** Biogeochemical tracers in the sediment model.

The three biogenic particles—organic carbon,  $\text{CaCO}_3$  and  $\text{bSiO}_2$ —and lithogenic clay become part of the sediment by sinking from the bottom seawater layer into the upper layer of the sediment. In reality, sedimentation (also called “rain” or “deposition”) creates new sediment on top of existing sediment, but in the model the sediment is defined on a fixed grid. The layer interfaces of the sediment are defined at 0, 0.1, 0.4, 0.9, 1.6, 2.5, 3.6, 4.9, 6.4, 8.1, 10.0, 12.1, 14.4 and 16.9 cm below the seawater–sediment interface. These define the twelve active layers, and one burial layer that stores all the particulate tracers that have been transported all the way down out of the active sediment domain. Typically, most of the sedimented material remineralises within the sediment; only a fraction of the biogenic compounds is buried. In the model, clay is considered inert and does not dissolve. In a steady state, burial equals sedimentation minus dissolution.

For each biogenic solid compound  $s$  there is at least one dissolved porewater component  $d$ . Within the sediment, these evolution equations hold:

$$\frac{dc_s}{dt} = \mathcal{B} \frac{\partial^2 c_s}{\partial z^2} - \frac{\partial}{\partial z} (w_s c_s) - \frac{v_{s \rightarrow d} M_s}{\rho(1 - \phi)} \quad (1a)$$

$$\frac{dc_d}{dt} = \frac{\partial}{\partial z} \left( \mathcal{D} \frac{\partial c_d}{\partial z} \right) + \frac{v_{s \rightarrow d}}{\phi}, \quad (1b)$$

where  $c_s$  is the weight fraction of compound  $s$  and  $c_d$  the porewater concentration of solute  $d$ ,  $\mathcal{B}$  is the diffusion coefficient for bioturbation,  $w_s$  the vertical advection velocity of the solid compounds,  $v$  the reaction rate,  $M_s$  the molecular weight of the solid compound,  $\rho$  the bulk sediment density,  $\phi$  is the porosity (the volume of the porewater divided by the total volume including the target solid sediment) and  $\mathcal{D}$  is the diffusion coefficient for porewater diffusion.

Sediment is displaced through bioturbation (Eq. 1a, RHS, 1st term) and vertical advection (2nd term) of solid constituents. Each of the last terms of Eqs 1a and 1b denotes decomposition of the solid components ( $s \rightarrow d$  conversion).

Organic matter, usually referred to as “organic carbon”, consists of many organic compounds of which the major ones are modelled. When organic matter remineralises, we assume

that all those compounds end up in dissolved phase simultaneously. In other words, in addition to the principal dissolved components  $d$  (phosphate for organic matter) from Eq. 1b there are other products  $d'$  (e.g. nitrate) that are created according to:

$$\frac{dc_{d'}}{dt} = R \frac{dc_d}{dt}, \quad (2)$$

where  $R$  is a stoichiometric expression, relating  $d'$  to  $d$ . Similarly, total alkalinity decreases as a consequence of organic carbon remineralisation and increases with the dissolution of calcium carbonate.

The porosity  $\phi$  is a prescribed function of depth, starting at 0.85 in the upper layer decreasing to 0.62 in the twelfth layer at around 13 cm depth. The rest of the volume,  $1 - \phi$ , is thus 0.15 at the surface and increases, through compactification, to 0.38 at 13 cm depth. In a filled state, this is the volume fraction of the bulk solid matter.

The model simulates the advection with respect to the sediment–water interface by shifting sediment vertically, depending on the “filling” state of the sediment. The total volume fraction occupied by solid material is given by the sum of the components’ volume fractions:

$$V_f = \sum_s \frac{M_s}{\rho_s} c_s, \quad (3)$$

where  $s$  runs over the four types of particulate matter,  $\rho_s$  is the density of the solid component (thus  $M_s/\rho_s$  the specific volume) and  $c_s$  the concentration. The shifting procedure sees to it that  $V_f$  approaches  $1 - \phi$ . If there is more deposition than remineralisation, sediment moves downwards at all depths to fill up the layers and the surplus created in the bottom layer of the active sediment (layer 12) is moved into the burial layer (layer 13). If there is not enough deposition relative to remineralisation, sediment moves upwards. To this end, the active sediment’s bottom layer will be overfilled from the burial layer with enough clay to fill the whole sediment. Then the layers above will be filled by redistribution (upward advection) from the surplus in layer 12.

### 2.1.3 Sediment–seawater burst coupling

In order to simulate a near-equilibrium of sediment biogeochemistry that is in agreement with the ocean circulation and biogeochemistry, we developed the so-called “burst-coupling” method. The model, BLOM/iHAMOCC, is adjusted such that we can choose to simulate the sediment processes alone while being forced by a seasonal climatology of bottom-seawater variables, or to couple the sediment with the rest of the ocean model. The variables include particle fluxes from the ocean onto the sediment and tracer concentrations. The fluxes define the sedimentation of biogenic and terrigenous particles. Dissolved tracer concentrations are used to calculate gradients between the porewater and overlying seawater for sediment–seawater fluxes. The climatology of the bottom-seawater variables consists of 12 mo and may be

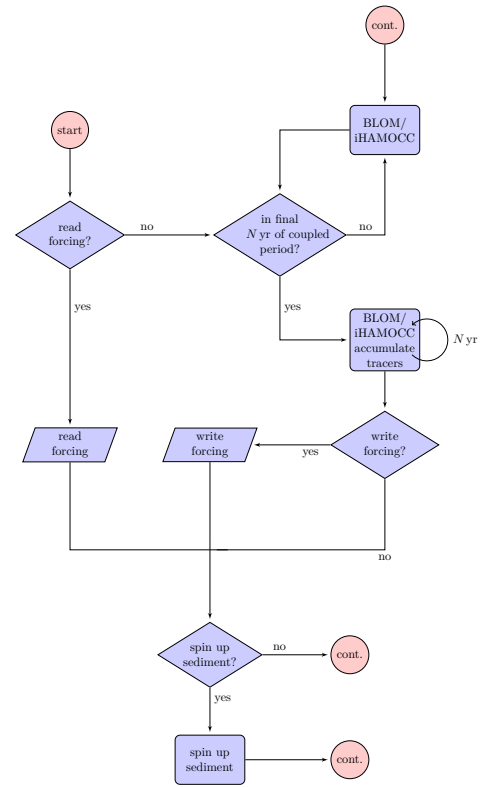


**Figure 1.** Flowchart of the burst coupling. The circles are connectors, the rectangles are processes and the rhomboids present input/output processing.

an average over a certain number of years at the end of the preceding coupled period.

Normally, a single iteration step for the sediment (finite difference approximation of the differential equations of Sec. 2.1.2) is performed for each water column biogeochemistry iteration, but in stand-alone mode a huge many iterations of the sediment are done (with a much larger timestep to speed up even more). These modes can be alternated in an automated manner where the user defines the coupled-mode and the decoupled-mode periods. Figure 1 shows the flowchart for this process.

If there is a bottom-seawater forcing present, it can be read from file. Otherwise, the simulation starts in coupled mode and a user-defined number of years are accumulated during all or the last part of the simulation (at least the last year) to derive a 12-month climatology. Optionally, this climatology is copied from volatile memory to file. Then the sediment is spun up decoupled. The process may be iterated by continuing the coupled simulation (with the spun-up sediment) and so on. The model terminates within the coupled mode when it reaches the user-defined number of coupled model years (standard NorESM configuration); this is not presented in this flowchart.

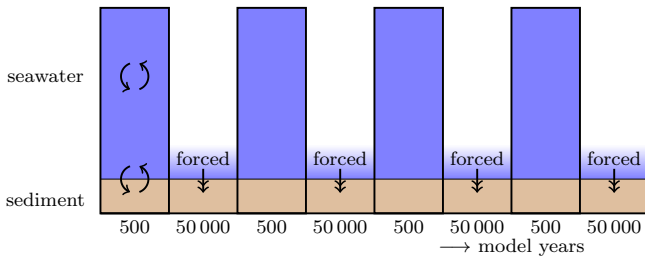


**Figure 2.** Burst coupling, a method to efficiently spin up a model consisting of a computationally slow and a fast component, where, in order to reach a steady state, the fast component needs to run many more model years than the slow component. In the depicted example, the coupled BLOM/iHAMOCC model that includes the computationally slow seawater component, is spun up for 250 yr, after which the fast sediment component is spun up for a much longer time. This may be repeated a couple of times, each time with a recent forcing.

### 2.1.4 Other improvements

Much of the code has been refactored and tidied up, which improved readability and computational performance (about 20 %). The details can be found in the commits, see <https://hg.gnu.org.ua/hgweb/burst-coupling/> and related discussion in Appendix C.

## 2.2 Simulations

We use a Holocene (pre-industrial) climate state. We first run the ocean model for 2000 yr, which is when the seawater tracers reach an approximate steady state (but still drift because of the unfilled sediment). Then we use the final state of this simulation as the initial conditions for the three different simulations that are listed in Table 2 and explained below. The time evolution of each of the simulations is presented in Fig. 3.

Name	Duration	Iterations
Coupled	1000 yr coupled	1
BurstShort	50 yr coupled, 400 yr sediment, 50 yr coupled	2
BurstLong	250 yr coupled, 50 kyr sediment	4

**Table 2.** Numerical simulations performed. All the simulation are forked from a 2000 yr coupled simulation, such that the water column is in an approximate steady state to start with.

- *Coupled* is a 1000-yr simulation where the water column and the sediment are coupled. Its purpose is that the other simulations can be compared to a base. Like the other simulations, it is preceded by a 2000-yr initial spin-up; so at the end of *Coupled*, the model has done 3000 yr of coupled integration.
- *BurstShort* has the same duration, but two intervals of it are sediment-only, decoupled from the water column and forced by bottom water particle fluxes and

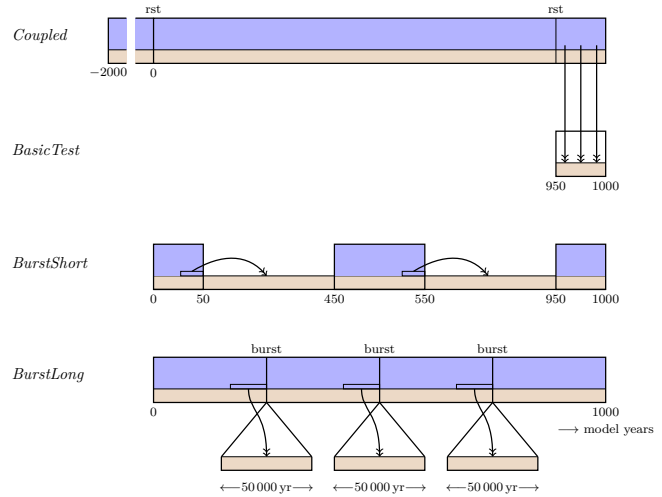


**Figure 3.** The model-time evolution of the four simulations (neither depth nor time are to scale). The blue areas represent the seawater and the brown the area below the seafloor (sediment and porewaters). The small rectangles in the lower-right corner of the seawater in the burst-coupling simulations represent the yearly averaged bottom-water climatology. The double arrows represent the forcing of off-line bottom-water variables onto the sediment.

tracer concentrations calculated from the last 50 yr of the preceding coupled simulation interval. This simulation tests if the method is basically working and if the sediment—when forced by a bottom-water climatology—is evolving sufficiently similar to *Coupled*. In other words, this shows how the water column forcing (in contrast to coupled mode) is affecting the sediment.

- *BurstLong* is a simulation of a total model duration of 151 000 yr. During the last 50 yr of an initial 250 yr coupled spin-up, the flux and tracer values are averaged over the duration each month and over the 50 yr. Then we run only the sediment model, decoupled from the rest of the model for 50 000 yr and forced by this climatology. This is iterated three times and finalised with another 250 yr of coupled integration (Fig. 2). By interleaving every 250 yr of coupled simulation with 50 kyr of sediment-only, we manage to make the total resulting coupled simulation 1000 yr. Hence we can analyse the effect of the long sediment bursts to the water column (compared to the 1000 yr of *Coupled*). Additionally, the simulation may give insight in how long an ocean model needs to spin up (without drifting because of sediment interaction).

## 2.3 Observations and evaluation

We use data from Archer (1996, 1999) to evaluate the  $\text{CaCO}_3$  and  $\text{bSiO}_2$  mass fractions in the sediment. Furthermore, the burial fluxes from Hayes et al. (2021) are used as a further criterion for the model performance.



### 3 Results

#### 3.1 Coupled simulation

In Figs 4–7 we present porewater and particle concentration development over the 2000 or 3000 yr spin-up of the coupled simulation. The figures show that the sediment is not filled with (most) particles within a couple of thousand years. For instance, in the Gulf of Panama  $\text{CaCO}_3$  appears to reach a dynamical equilibrium after about 1000 yr in the upper layers of the sediment (upper 2.5 cm), but at higher depths (below 6.4 cm) it will take notably longer than 2000 yr for  $\text{CaCO}_3$  to reach a steady state (Fig. 4). Only  $\text{bSiO}_2$  looks in a steady state from the start, or maybe from about 500 yr.

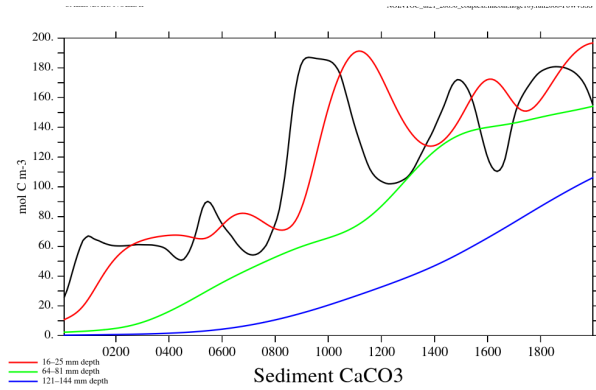


**Figure 4.**  $\text{CaCO}_3$  timeseries at different depths in the sediment of *Coupled* in the Gulf of Panama ( $80^\circ \text{ W}$ ,  $5^\circ \text{ N}$ ).

This alone warrants a relatively long spin-up of at least the sediment. Even if one is not interested in the sediment, it should be realised that the interaction of the seawater with a changing (non-steady state) sediment will lead to a drift in an ocean- or climate model. Of course a priori reasoning is not enough to conclude if such a drift is significant.

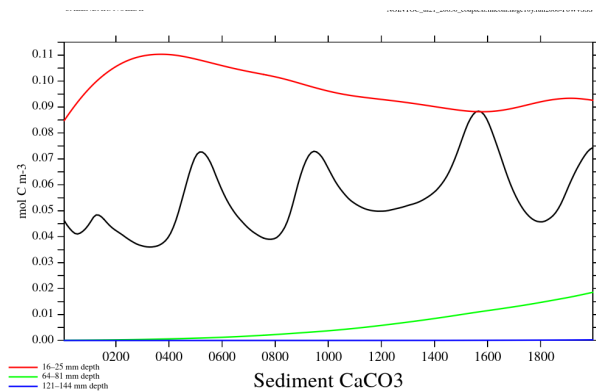


**Figure 5.**  $\text{CaCO}_3$  timeseries at different depths in the sediment of *Coupled* at MANOP site S ( $140^\circ \text{ W}$ ,  $11.33^\circ \text{ N}$ ).

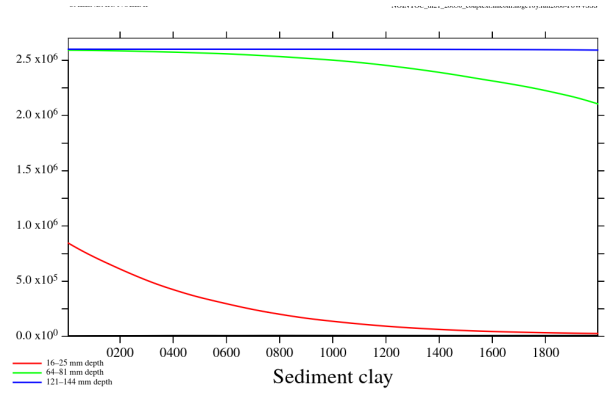


**Figure 6.** Clay timeseries at different depths in the sediment of *Coupled* at MANOP site S ( $140^\circ \text{ W}$ ,  $11.33^\circ \text{ N}$ ).

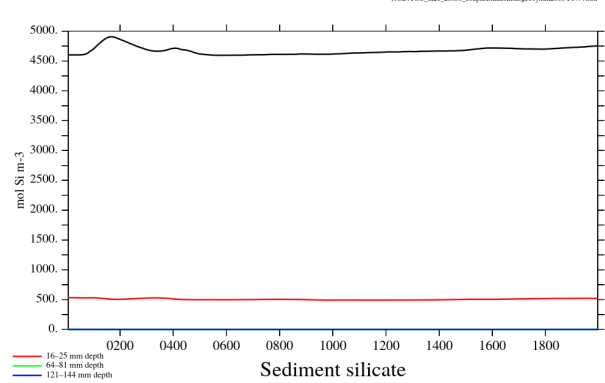


**Figure 7.**  $\text{bSiO}_2$  timeseries at different depths in the sediment of *Coupled* in the Gulf of Panama ( $80^\circ \text{ W}$ ,  $5^\circ \text{ N}$ ).

#### 3.2 Global spin-up evolution

We present the timeseries of  $\text{CaCO}_3$  (sediment average) of the *BurstLong* simulation (Fig. 8). It shows the 1000 yr of coupled simulation, interleaved with the three 50 000 yr of

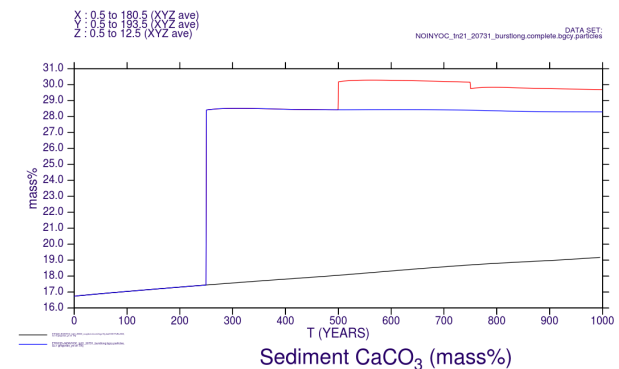


**Figure 8.** Modelled  $\text{CaCO}_3$  timeseries in the sediment (global average, upper 14.4 cm): black is 1000 yr of coupled, blue includes one sediment-only period of 50 000 yr, red includes three such burst periods.

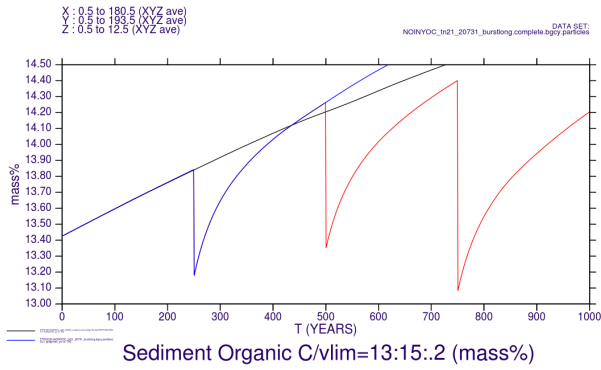


**Figure 9.** Modelled OC timeseries in the sediment (global average, upper 14.4 cm): black is 1000 yr of coupled, blue includes one sediment-only period of 50 000 yr, red includes three such burst periods. See Fig. 10 for the timeseries including the 50 000 yr decoupled bursts (albeit compressed).

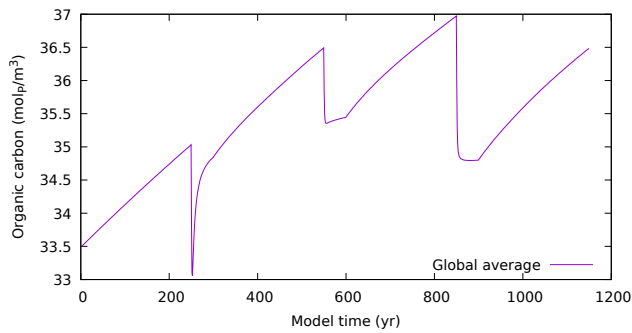
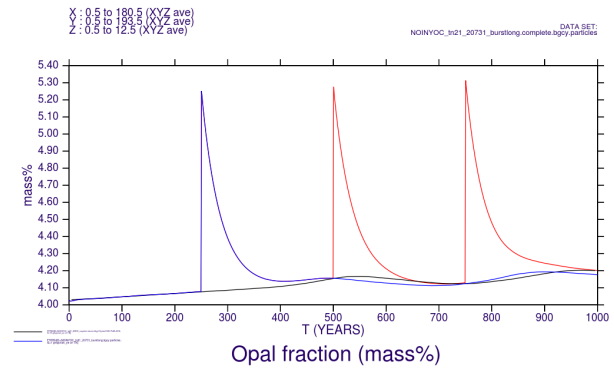


**Figure 10.** Modelled OC timeseries in the sediment (global average, upper 14.4 cm) from *BurstLong*. The time axis of the 50 000 yr burst periods are compressed by a factor of 1000.

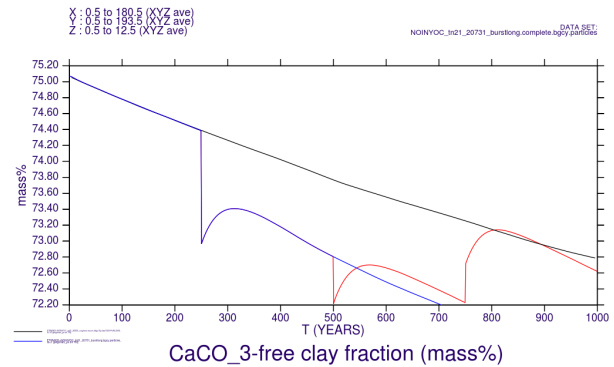
decoupled sediment simulation. The figure shows that at least two sediment-only burst periods are needed to get the sediment in a steady state, and subsequent bursts have less and less influence. The bursts have a significant effect for the other particles as well, as can be seen in Figs 9–12. However, after each burst there is a relaxation towards the mass fractions of the coupled simulation (*Coupled*). The relative change over the whole simulation time is much smaller for organic carbon (Fig. 9) and bSiO<sub>2</sub> (Fig. 11) than for CaCO<sub>3</sub>, and the deviation by the bursts could just be contingent upon the forcing integrated.

Fig. 13 shows a 50 kyr burst, again from *BurstLong*, where the sediment content of CaCO<sub>3</sub> approaches a steady state. In the subsequent figure (Fig. 14), organic carbon is plotted for the same stand-alone sediment simulation. In addition, also a region in the eastern Central Pacific is plotted where there is a high flux of organic carbon (as well as biogenic silica).

As expected, during the 50-kyr sediment-only simulations immediately after years 250, 500 and 750 of the coupled simulation, much more burial occurs than during any of the



**Figure 11.** Modelled bSiO<sub>2</sub> timeseries in the sediment (global average, upper 14.4 cm): black is 1000 yr of coupled, blue includes one sediment-only period of 50 000 yr, red includes three such burst periods.



**Figure 12.** Modelled clay timeseries in the sediment (global average, upper 14.4 cm): black is 1000 yr of coupled, blue includes one sediment-only period of 50 000 yr, red includes three such burst periods.

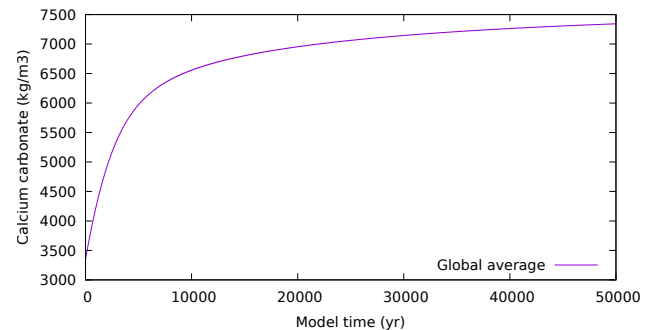


**Figure 13.** Modelled CaCO<sub>3</sub> timeseries in the sediment (average over upper 14.4 cm) of the first ‘burst’ of 50 000 yr.

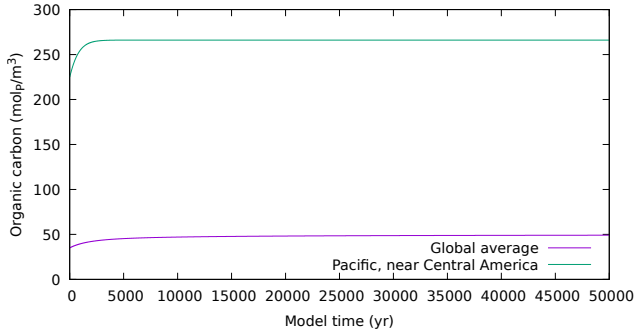


**Figure 14.** Modelled organic carbon ( $\text{mol}_P \text{m}^{-3}$ ) timeseries in the sediment (average over upper 14.4 cm) of the first ‘burst’ of 50 000 yr. In addition to a global average the figure also shows the timeseries of the high particle flux region just west of Central America.

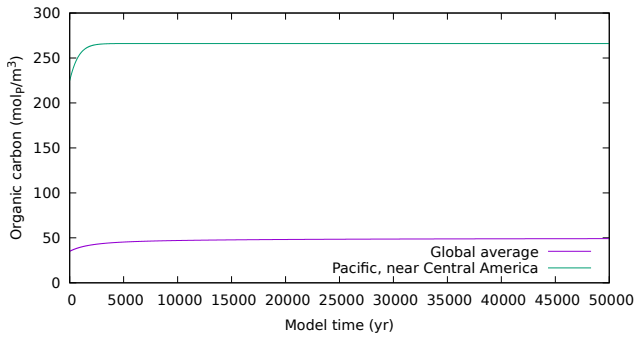


**Figure 15.** Modelled organic carbon ( $\text{mol}_P \text{m}^{-3}$ ) timeseries in the sediment (average over upper 14.4 cm) of the full 1000+150 000 yr simulation. The duration during the decoupled periods each 250 yr is compressed such that one year on the x-axis represents 1000 yr in model time.

250-yr periods. We present the average molar concentration timeseries of organic matter in Fig. 15. Organic carbon changes only slightly during the 1000 yr coupled + 150 kyr sediment-only simulation, from  $33.5 \text{ mol}_P \text{m}^{-3}$  to  $36.5 \text{ mol}_P \text{m}^{-3}$ . During coupled simulation, organic carbon increases (but the second derivative is negative). During sediment-only simulation, organic carbon decreases.

### 3.2.1 Effect on water column

Figs 16–18 show globally averaged quantities in the water column from *Coupled* and *BurstLong*. In all the figures from year 250, where the first decoupled period takes place, the behaviour of *BurstLong* (black line) is accelerated in both magnitude and phase. Of course the effect is much more moderate than for the tracers in the sediment, but the 50 000 yr spin-up of the sediment clearly has an effect on the water column tracers. It is a small effect compared to the absolute value ( $< 1\%$ ) but large compared to centennial variability ( $> 20\%$ ).

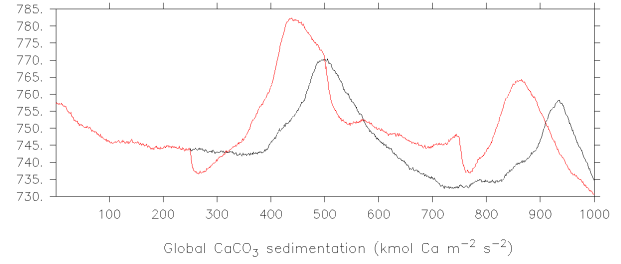


**Figure 16.**  $\text{CaCO}_3$  global flux at the ocean bottom (sedimentation); against time (yr). The black line is the final 1000 yr of *Coupled*; the red line represents *BurstLong*.

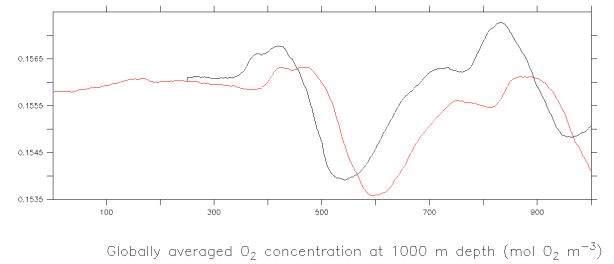


**Figure 17.**  $\text{O}_2$  concentration at 1000 m depth; global average; against time (yr). The red line is the final 1000 yr of *Coupled*; the black line represents *BurstLong*.

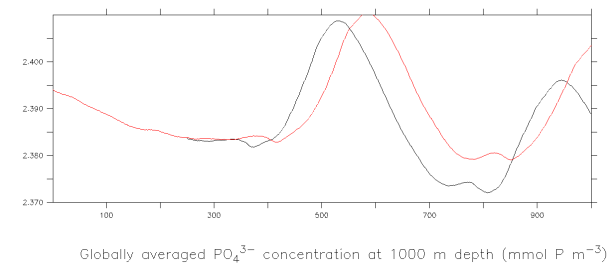


**Figure 18.**  $\text{PO}_4^{3-}$  concentration at 3000 m depth; global average; against time (yr). The red line is the final 1000 yr of *Coupled*; the black line represents the burst coupling with decoupled 50 kyr periods every 250 yr.

### 3.3 Verification of the method

*BurstShort* would measure the effect of forcings on the sediment compared to *Coupled*. We have not finished this analysis. Instead we will show the results of a ‘synchronous’ simulation, named *BasicTest*. That simulation takes only 51 yr of which 50 yr forced by the respective stored bottom water variables of *Coupled* (see Fig. 3). As such we will, in a way, more precisely track the deviation from the coupled simulation based on (about) the best presentation of bottom water forcings that we can get while still using a full stored year.

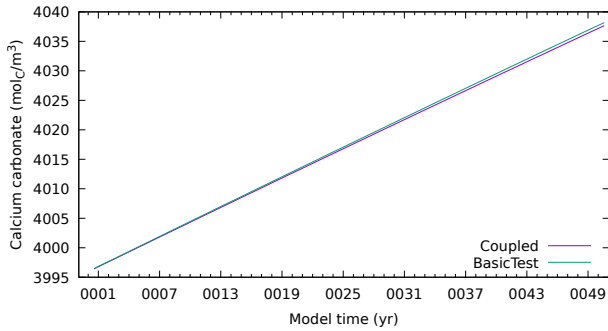


**Figure 19.**  $\text{CaCO}_3$  molar concentration in the sediment of the last 51 yr of the simulations *Coupled* and *BasicTest*.

Figs 19 and 20 present the timeseries of the globally averaged sediment concentration of  $\text{CaCO}_3$  and  $\text{bSiO}_2$  of *Coupled* together with *BasicTest*. At the start of the simulations the concentration coincided for both tracers. Then both tracers in *BasicTest* start to deviate from *Coupled*. After 50 yr, calcium carbonate has deviated about 0.01 %, whereas biogenic silica has deviated about 1.4 %.

The water column concentrations did not change during the stand-alone sediment simulation and continued spinning up only in the coupled periods (not further presented).

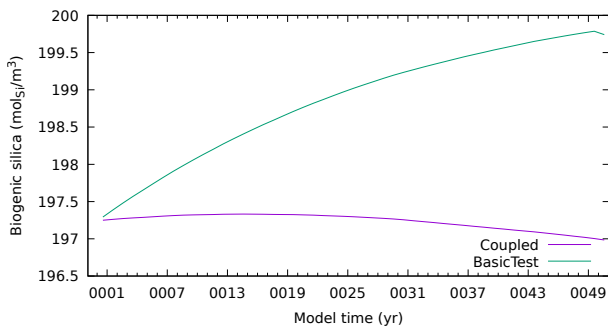


**Figure 20.**  $\text{bSiO}_2$  molar concentration in the sediment of the last 51 yr of the simulations *Coupled* and *BasicTest*.

### 3.4 Evaluation

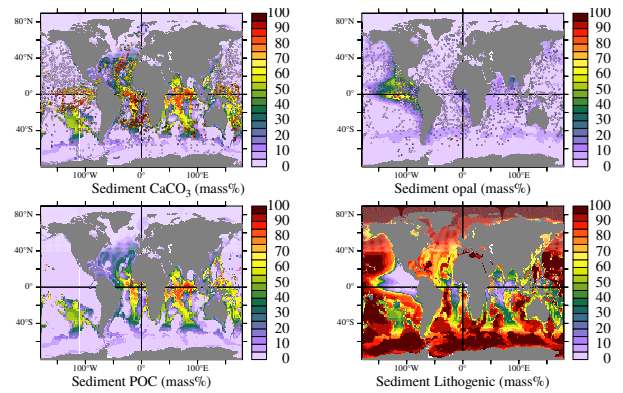
This report will not show a full evaluation of the model that, amongst other things, would compare the 151 000 yr simulation (*BurstLong*) against observations. We have shown in the previous two subsections that our method works. For a more complete evaluation of BLOM/iHAMOCC we refer to the analysis in the recent coupled CMIP6 NorESM simulations (Tjiputra et al., 2020). One of the goals of our study was to show if a spun up sediment has an effect on the ocean state and we have indications that it has.

#### 3.4.1 Pelagic zone

BLOM/iHAMOCC has been evaluated by Tjiputra et al. (2020), but this is mostly limited to the upper part of the water column. Moreover, they had spun up the model in the order of 1000 yr to a quasi steady state. As expected, most variables in the seawater from our *BurstLong* simulation are similar to those in Tjiputra et al. (2020). The deepest part of the ocean and especially the sediment were not in a steady state or not analysed. Hence we will here evaluate a few features of the spun up model, mostly using the average of the final part of *BurstLong*.

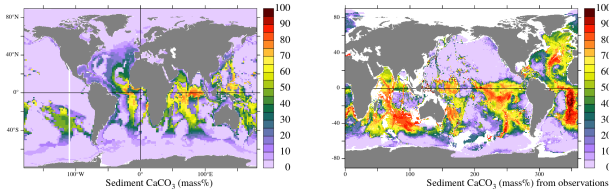
#### 3.4.2 Benthic zone and seabed

Figure 21 presents the particle composition of the sediment according to our model.



**Figure 21.** Particle composition of the sediment, average over depth and the last 1000 yr of a 251 kyr burst-coupled simulation. The calcium carbonate and biogenic silica data—plotted as discs on the same colour scale—are from Archer (1996) (revised dataset at Archer (1999)).

In Figure 22(b) observations by Archer (1996) are presented. The model underestimates  $\text{CaCO}_3$  concentrations at most places, and especially in the equatorial East Pacific. The northern Indian Ocean is reasonably represented, not the southern part. The low  $\text{CaCO}_3$  fraction in the Southern Ocean, however, is well represented. This was expected as this is likely to rather contain opal instead of calcium carbonate. The simulation shows high concentrations of lithogenic material in especially the Southern and Arctic Oceans. Even



**Figure 22.** Mass fraction of calcium carbonate according to our model, and from core-top data (Archer, 1996).

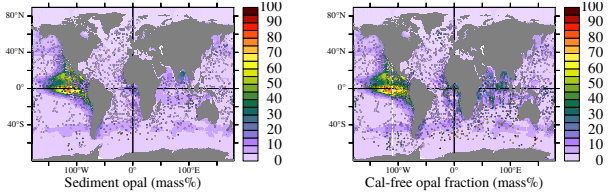


**Figure 23.** bSiO<sub>2</sub> fraction of the sediment, average over full model active sediment depth (0–15 cm) and the last 1000 yr of a 251 kyr burst-coupled simulation. The biogenic silica data—plotted as discs on the same colour scale—are from Archer (1996) (revised dataset at Archer (1999)). **Left:** relative to total particulate; **right:** relative to particles excluding CaCO<sub>3</sub>.

though the opal belt is reproduced by the model (Section 3.4.1 and Tjiputra et al. (2020)), the sedimentary biogenic silica fraction is nonetheless underestimated.

The POC at the Patton Escarpment (Fig. 28, left panel) has the right asymptotic order of magnitude, 0.8 % compared with 1.4 % from observations (Sarmiento and Gruber, 2006, p. 231), but the shape is wrong (starting at the surface below 0.5 % at the surface instead of 1.7 % in observations). The seawater profiles (Fig. 27) show some consistency in that the highest concentration near the bottom are in the right panel (Panama, where we expect high organic particle loads), consistent with the about 6 % in the sediment. Of course, percentages cannot be directly compared with concentrations; it depends also on the other particles' sedimentation. The zero value in the middle panel of the sediment profiles is inconsis-

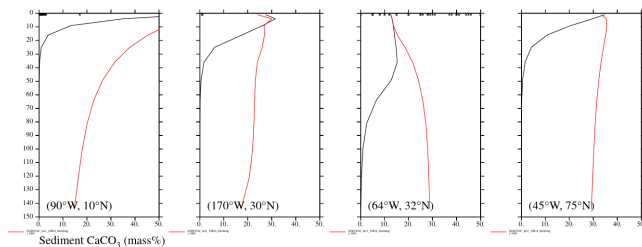


**Figure 24.** Profiles of CaCO<sub>3</sub> in the eastern equatorial Pacific Ocean, central North Pacific, BATS station and Weddell Sea. The vertical axis is the sediment depth (mm); the horizontal mass fraction of CaCO<sub>3</sub>. The black line is after 1000 yr of normal BLOM/iHAMOCC simulation (*Coupled*); the red line is also 1000 yr but every 250 yr the sediment is decoupled to run 100 kyr stand-alone, (*BurstLong*).

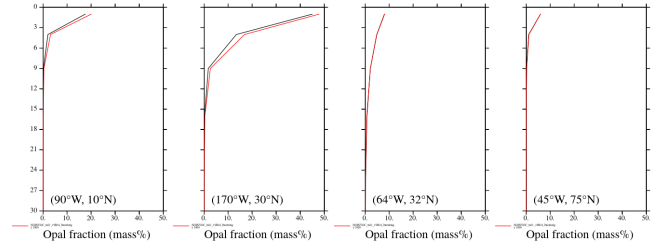


**Figure 25.** Profiles of bSiO<sub>2</sub> in the eastern equatorial Pacific Ocean, central North Pacific, BATS station and Weddell Sea. The vertical axis is the sediment depth (only upper 30 mm); the horizontal mass fraction of bSiO<sub>2</sub>. The black line is after 1000 yr of normal BLOM/iHAMOCC simulation (*Coupled*); the red line is also 1000 yr but every 250 yr the sediment is decoupled to run 100 kyr stand-alone, (*BurstLong*).

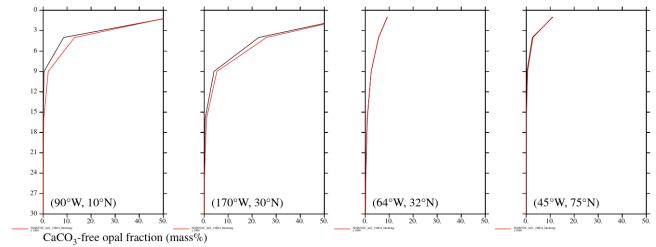


**Figure 26.** Profiles of the calcium carbonate free mass fraction of bSiO<sub>2</sub> in the eastern equatorial Pacific Ocean, central North Pacific, BATS station and Weddell Sea. The vertical axis is the sediment depth (only upper 30 mm); the horizontal mass fraction of bSiO<sub>2</sub>. The black line is after 1000 yr of normal BLOM/iHAMOCC simulation (*Coupled*); the red line is also 1000 yr but every 250 yr the sediment is decoupled to run 100 kyr stand-alone, (*BurstLong*).

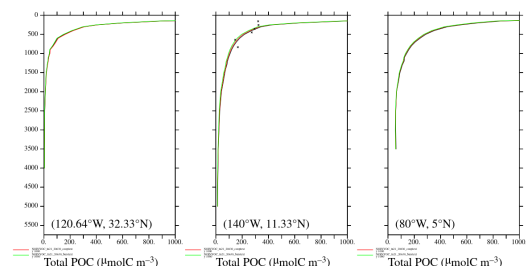


**Figure 27.** Profiles of the POC concentration in the Pacific Ocean seawater. From left to right: the Patton Escarpment, MANOP Site S, and the Gulf of Panama. The vertical axis is the water column depth (m). The black line is after 1000 yr of normal BLOM/iHAMOCC simulation (*Coupled*); the red line after 1672 year; and the green line is after 1000 yr plus and additional 1000 yr coupled burst coupled, interrupted by decoupled sediment simulations of run 50 kyr stand-alone (*BurstLong*). The crosses are measurements from Lam et al. (2011).



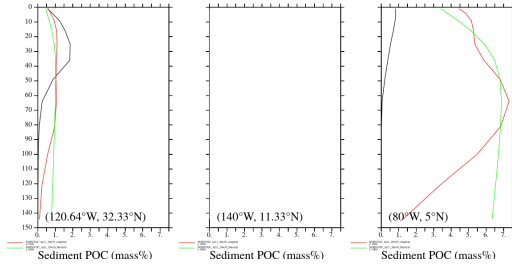


**Figure 28.** Profiles of the mass fraction of POC in the Pacific Ocean. From left to right: the Patton Escarpment, MANOP Site S, and the Gulf of Panama. The vertical axis is the sediment depth (mm). The black line is after 1000 yr of normal BLOM/iHAMOCC simulation (*Coupled*); the red line after 1672 year; and the green line is after 1000 yr plus and additional 1000 yr coupled burst coupled, interrupted by decoupled sediment simulations of run 50 kyr stand-alone (*BurstLong*).

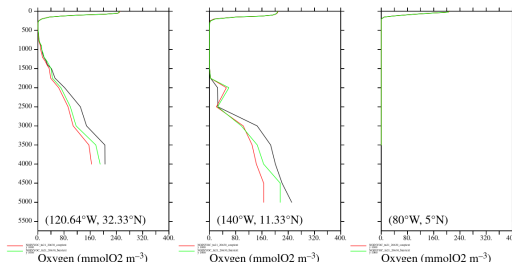


**Figure 29.** Profiles of the porewater concentration of  $O_2$  in the Pacific Ocean seawater. From left to right: the Patton Escarpment, MANOP Site S, and the Gulf of Panama. The vertical axis is the water column depth in m. The black line is after 1000 yr of normal BLOM/iHAMOCC simulation (*Coupled*); the red line after 1672 year; and the green line is after 1000 yr plus and additional 1000 yr coupled burst coupled, interrupted by decoupled sediment simulations of run 50 kyr stand-alone (*BurstLong*).

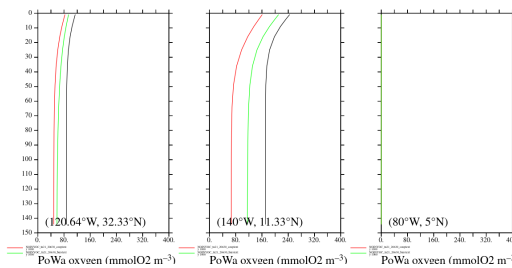


**Figure 30.** Profiles of the porewater concentration of  $O_2$  in the Pacific Ocean. From left to right: the Patton Escarpment, MANOP Site S, and the Gulf of Panama. The vertical axis is the sediment depth in mm. The black line is after 1000 yr of normal BLOM/iHAMOCC simulation (*Coupled*); the red line after 1672 year; and the green line is after 1000 yr plus and additional 1000 yr coupled burst coupled, interrupted by decoupled sediment simulations of run 50 kyr stand-alone (*BurstLong*).

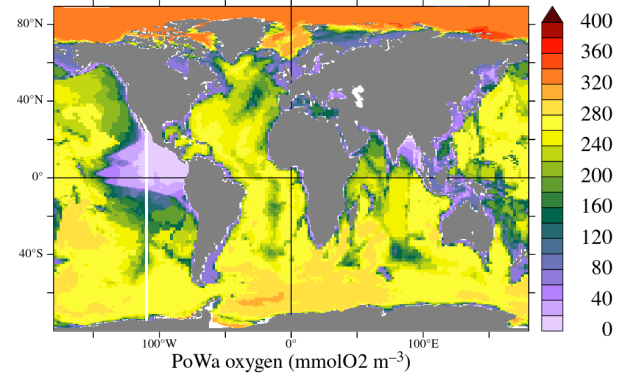


**Figure 31.** The depth-averaged porewater concentration of  $O_2$  in the World Ocean. Yearly average at the end of *BurstLong*.

Type of particle	Global burial rate			
	Tmol/yr	% <sub>&gt;200m</sub>	Tg/yr	Tg/yr
Organic carbon	28 C	63	337 C	843 $C_6H_{12}O_6$
Calcium carbonate	26 C	91	318 C	2649 $CaCO_3$
Biogenic silica	23 Si	29	644 Si	1375 $SiO_2$
Clay mineral	1.15	84	1.15	1.15

**Table 3.** The burial rates after the 251 kyr simulation of *BurstLong*.

tent with the particles in the seawater (latter compares well with observations).

The oxygen profiles in the seawater (Fig. 29) and the sediment (Fig. 30). Oxygen concentrations are practically zero in the Gulf of Panama (see also the map of Fig. 31). The sediment profiles have the right basic shape (Sarmiento and Gruber, 2006, p. 231), but they don't become zero at the Patton Escarpment (continental margin, left panel of Fig. 30). This can of course be because of the too low resolution of the model to resolve the continental margin. The depth-average oxygen concentration in the sediment shows the hypoxic/anoxic areas around continents.

The burial rates from near the end of the 251 kyr simulation of *BurstLong* are given in Table 3.

Estimates of burial have a large variance. For calcium carbonate the burial ranges typically from 100  $Tg_C yr^{-1}$  to 150  $Tg_C yr^{-1}$  (Cartapanis et al., 2018). The model yields a burial that is more than two times higher than their upper limit. Then again, earlier estimates of  $CaCO_3$  burial were higher and much closer to our result (Milliman, 1993; Milliman and Droxler, 1996). In the model, when calcium carbonate is undersaturated, it dissolves following a first-order dissolution. The dissolution rate constant may be adjusted, and a higher-rate dissolution parameterisation could be considered as well (e.g. Subhas et al., 2015). Recent estimates of biogenic silica burial are  $(202 \pm 115) Tg_{Si} yr^{-1}$  (Tréguer and De La Rocha, 2013), whereas our model yields a factor of three higher burial rate. Also our carbon burial is overestimated with a factor of three. Compare iHAMOCC's

$337 \text{ Tg}_C \text{ yr}^{-1}$  with  $112 \text{ Tg}_C \text{ yr}^{-1}$  (Dunne et al., 2007) and  $156 \text{ Tg}_C \text{ yr}^{-1}$  (Burdige, 2007).

The coupled simulation (*Coupled*) shows a relatively continuous rise of particle content, because the sediment is filling up. The burial is close to zero at the beginning of the simulation, because no particles are present yet in the bottom sediment layer. After burst coupling (*BurstLong*), the sediment is spun up and fluxes are much higher and without any obvious trend.

### 3.5 Runtime efficiency

Using the burst-coupling method we reached a model performance increase per model year of about a factor of 19. This is on top of an about 20 % performance gain because of the refactoring done to the code before and during implementation of the burst-coupling method.

## 4 Discussion and conclusion

A complete steady state is only reached for  $\text{CaCO}_3$  and POC far beyond 100 000 yr, suggesting that (1) models that are similar in the relevant respects need such a long spin-up and (2) the real ocean needs more than 100 000 yr to equilibrate. In reality this may be shorter.

One issue with determining the equilibration time is the choice of the coupling/decoupling procedure. Instead of one parameter (time), it introduces three independent parameters, namely coupled time, decoupled time and the number of iterations (or total integration time).<sup>1</sup> The 50 000 yr of stand-alone sediment integration is very long, chosen for the practical reason that the sediment module integrates very fast, so why not spin it up to a near steady state. A consequence of our model setup is that the total integration time may not be a good measure for how long an ocean model needs to get in whack.

Moreover, it appears that the full ocean system in *Burst-Long* is not yet quite in whack and needs at least a couple more iterations. This is, abducting from the previous paragraph, due to too little coupled integration time.

Our model underestimates the sediment calcium carbonate mass fraction, especially in the equatorial Pacific (Fig 21 or 22). The general distribution patterns of calcium carbonate are realistic; they relate to the topography as the observations. The biogenic silica is underestimated in the opal belt and overestimated in the equatorial Pacific. It seems that in the model diatoms rule in the equatorial Pacific, but in reality coccolithophores are important there. Also carbon burial is likely strongly overestimated and hence pressing the calcium carbonate mass fraction burial.

<sup>1</sup>One could deviate from our model scheme by allowing variable coupled or decoupled periods, allowing for instance to change the coupling state as soon as the relevant ocean component approaches a steady state. One might also use a climatology from one based on the last 50 yr of a coupled simulation; this should consider the extend of interyearly variability.

Overall burial of all particles in iHAMOCC could be increased by increasing the bioturbation coefficient that is not well known. This would speed up the burial process (e.g. Boudreau, 1997, pp. 41–44). It is not known if the bioturbation of  $1 \times 10^{-9} \text{ m}^2 \text{ s}^{-1}$  that we used is realistic.

## 5 Code availability

The sediment burst-coupling code may be obtained at <https://puszcza.gnu.org.ua/projects/burst-coupling/>. For this study, different revisions of the code from 105:fe270f4aa7db to 121:dad56c57eb86 were used. The repository also contains a manual for using burst coupling with BLOM/iHAMOCC. The mathematical variable names correspond to the Fortran variables as described in Table A1 in the appendix.

Analysis scripts can be found at <https://hg.sr.ht/~marco/sediment-analysis>. A short manual for using these scripts can be found in Appendix B. Model output is available on request.

## 6 Authors' contributions

The model and the simulations were designed by MvH, JS, JT and CH. MvH designed the burst coupling code structure with contributions from JS, JT, CH, MB and AG. The manuscript was prepared by MvH with close collaboration and major contributions from CH, JS, and JT.

The authors declare that they have no conflict of interest.

**Acknowledgements.** We would like to thank Mats Bentsen for the useful discussions about the model design. We thank Alok Gupta and Anne Morée for helping with the model setup.

This study was supported by the project “Overturning circulation and its implications for the global carbon cycle in coupled models” (ORGANIC, The Research Council of Norway, grant No. 239965). This work was also supported through project CRESCENDO (Co-ordinated Research in Earth Systems and Climate: Experiments, Knowledge, Dissemination and Outreach; Horizon 2020 European Union’s Framework Programme for Research and Innovation, grant No. 641816, European Commission).

The authors wish to acknowledge the use of Ferret, a product of NOAA’s Pacific Marine Environmental Laboratory. The plots in this paper were created by the Ferret visualisation library ComPlot (Van Hulten, 2017) and gnuplot.

## References

- Archer, D. and Maier-Reimer, E.: Effect of deep-sea sedimentary calcite preservation on atmospheric  $\text{CO}_2$  concentration, *Nature*, 367, 260–263, <https://doi.org/10.1038/367260a0>, 1994.
- Archer, D. E.: An atlas of the distribution of calcium carbonate in sediments of the deep sea, *Global Biogeochem. Cy.*, 10, 159–174, <https://doi.org/10.1029/95GB03016>, data at: <https://doi.org/10.1594/PANGAEA.56017>, 1996.



- Archer, D. E.: Opal, quartz and calcium carbonate content in surface sediments of the ocean floor, <https://doi.org/10.1594/PANGAEA.56017>, data at: <https://doi.org/10.1594/PANGAEA.56017>, 1999.
- Bentsen, M., Bethke, I., Debernard, J. B., Iversen, T., Kirkevåg, A., Seland, Ø., Drange, H., Roelandt, C., Seierstad, I. A., Hoose, C., and Kristjánsson, J. E.: The Norwegian Earth System Model, NorESM1-M – Part 1: Description and basic evaluation of the physical climate, *Geosci. Model Dev.*, 6, 687–720, <https://doi.org/10.5194/gmd-6-687-2013>, 2013.
- Boudreau, B. P.: Diagenetic Models and Their Implementation, Springer, 1997.
- Burdige, D. J.: Preservation of Organic Matter in Marine Sediments: Controls, Mechanisms, and an Imbalance in Sediment Organic Carbon Budgets?, *Chem. Rev.*, 107, 467–485, <https://doi.org/10.1021/cr050347q>, 2007.
- Cartapanis, O., Galbraith, E., Bianchi, D., and Jaccard, S.: Carbon burial in deep-sea sediment and implications for oceanic inventories of carbon and alkalinity over the last glacial cycle, *Clim. of the Past*, 14, 1819–1850, <https://doi.org/10.5194/cp-14-1819-2018>, 2018.
- Dunne, J. P., Sarmiento, J. L., and Gnanadesikan, A.: A synthesis of global particle export from the surface ocean and cycling through the ocean interior and on the seafloor, *Global Biogeochem. Cy.*, 21, <https://doi.org/10.1029/2006GB002907>, gB4006, 2007.
- Hasselmann, K.: How well can we predict the Climate Crisis?, in: ENVIRONMENTAL SCARCITY. THE INTERNATIONAL DIMENSION, [https://pure.mpg.de/rest/items/item\\_2536177/component/file\\_2536176/content](https://pure.mpg.de/rest/items/item_2536177/component/file_2536176/content), 1991.
- Hayes, C. T., Costa, K. M., Calvo, E. M., Chase, Z., Demina, L. L., Dutay, J.-C., German, C. R., Heimbürger-Boavida, L.-E., Jaccard, S. L., Jacobel, A., Kohfeld, K. E., Kravchishina, M. D., Lippold, J., Mekik, F., Missiaen, L., Pavia, F., Paytan, A., Petrova, M. V., Pedrosa-Pàmies, R., Rahman, S., Robinson, L. F., Roy-Barman, M., Sánchez-Vidal, A., Shiller, A. M., Tagliabue, A., Tessin, A. C., van Hulten, M., and Zhang, J.: The Composition and Flux of Seafloor Sediments in the Global Ocean, *Global Biogeochem. Cycles*, 35, e2020GB006769, <https://doi.org/10.1029/2020GB006769>, 2021.
- Heinze, C., Hoogakker, B. A. A., and Winguth, A.: Ocean carbon cycling during the past 130 000 years – a pilot study on inverse palaeoclimate record modelling, *Clim. of the Past*, 12, 1949–1978, <https://doi.org/10.5194/cp-12-1949-2016>, 2016.
- Hulten, M.M.P. van: Aluminium and Manganese in the West Atlantic Ocean, Ph.D. thesis, University of Groningen, <http://irs.ub.rug.nl/ppn/384091636>, printed version available on request to the author, 2014.
- Hulten, M.M.P. van: ComPlot: Comparison Plotter to visually evaluate ocean model simulations, *J. Open Source Softw.*, 2, <https://doi.org/10.21105/joss.00368>, 2017.
- IPCC: Sixth Assessment Report: Climate Change 2022, Cambridge University Press, <https://www.ipcc.ch/report/sixth-assessment-report-working-group-i/>, 2021.
- Kirkevåg, A., Iversen, T., Seland, Ø., Hoose, C., Kristjánsson, J. E., Struthers, H., Ekman, A. M. L., Ghan, S., Griesfeller, J., Nilsson, E. D., and Schulz, M.: Aerosol–climate interactions in the Norwegian Earth System Model NorESM1-M, *Geosci. Model Dev.*, 6, 207–244, <https://doi.org/10.5194/gmd-6-207-2013>, 2013.
- Lam, P. J., Doney, S. C., and Bishop, J. K. B.: The dynamic ocean biological pump, *Global Biogeochem. Cy.*, 25, GB3009, <https://doi.org/10.1029/2010GB003868>, 2011.
- Maier-Reimer, E., Kriest, I., Segschneider, J., and Wetzel, P.: The HAMburg Ocean Carbon Cycle model HAMOCC5.1 – technical description release 1.1, Tech. rep., 2005.
- Milliman, J. D.: Production and accumulation of calcium carbonate in the ocean: Budget of a nonsteady state, *Global Biogeochem. Cy.*, 7, 927–957, <https://doi.org/10.1029/93GB02524>, 1993.
- Milliman, J. D. and Droxler, A. W.: Neritic and pelagic carbonate sedimentation in the marine environment: ignorance is not bliss, *Geologische Rundschau*, 85, 496–504, <https://doi.org/10.1007/BF02369004>, 1996.
- Sabine, C., Feely, R., Gruber, N., Key, R., Lee, K., Bullister, J., Wanninkhof, R., Wong, C., Wallace, D., Tilbrook, B., et al.: The oceanic sink for anthropogenic CO<sub>2</sub>, *Science*, 305, 367, <https://doi.org/10.1126/science.1097403>, 2004.
- Sarmiento, J. and Gruber, N.: Ocean Biogeochemical Dynamics, Princeton University Press, 2006.
- Schwinger, J., Goris, N., Tjiputra, J. F., Kriest, I., Bentsen, M., Bethke, I., Ilıcak, M., Assmann, K. M., and Heinze, C.: Evaluation of NorESM-OC (versions 1 and 1.2), the ocean carbon-cycle stand-alone configuration of the Norwegian Earth System Model (NorESM1), *Geosci. Model Dev.*, 9, 2589–2622, <https://doi.org/10.5194/gmd-9-2589-2016>, 2016.
- Steinfeldt, R., Rhein, M., Bullister, J. L., and Tanhua, T.: Inventory changes in anthropogenic carbon from 1997–2003 in the Atlantic Ocean between 20°S and 65°N, *Global Biogeochem. Cy.*, 23, <https://doi.org/10.1029/2008GB003311>, 2009.
- Subhas, A. V., Rollins, N. E., Berelson, W. M., Dong, S., Erez, J., and Adkins, J. F.: A novel determination of calcite dissolution kinetics in seawater, *Geochim. Cosmochim. Ac.*, 170, 51–68, <https://doi.org/10.1016/j.gca.2015.08.011>, 2015.
- Takahashi, T., Broecker, W. S., and Langer, S.: Redfield ratio based on chemical data from isopycnal surfaces, *J. Geophys. Res.*, 90, 6907–6924, <https://doi.org/10.1029/JC090iC04p06907>, 1985.
- Tjiputra, J. F., Schwinger, J., Bentsen, M., Morée, A. L., Gao, S., Bethke, I., Heinze, C., Goris, N., Gupta, A., He, Y., Olivié, D., Seland, Ø., and Schulz, M.: Ocean biogeochemistry in the Norwegian Earth System Model version 2 (NorESM2), *Geosci. Model Dev.*, 13, 2393–2431, <https://doi.org/10.5194/gmd-13-2393-2020>, 2020.
- Tréguer, P. and De La Rocha, C.: The World Ocean Silica Cycle, *Annu. Rev. Mar. Sci.*, 5, <https://doi.org/10.1146/annurev-marine-121211-172346>, 2013.

## Appendix A: Model variables

Symbol	Description	Value	Unit	Code
<i>state variables of the solid fraction (s)</i>				
$c_s$	Concentration of solid sediment component $s$	Variable	concentration	sedlay(:, :, :, :)
OC	Organic carbon	Variable	$\text{mol}_P \text{ dm}^{-3}$	sedlay(:, :, :, issso12)
$\text{CaCO}_3$	Calcium carbonate	Variable	$\text{mol}_C \text{ dm}^{-3}$	sedlay(:, :, :, isssc12)
$\text{bSiO}_2$	Biogenic silica	Variable	$\text{mol}_{Si} \text{ dm}^{-3}$	sedlay(:, :, :, issssil)
clay	lithogenic (via dust)	Variable	$\text{kg m}^{-3}$	sedlay(:, :, :, issster)
<i>state variables of the porewater (d)</i>				
$c_d$	Concentration of dissolved porewater component $d$	Variable	molar concentration	powtra(:, :, :, :)
DIC	Dissolved inorganic carbon	Variable	$\text{mol}_C \text{ dm}^{-3}$	powtra(:, :, :, ipowaic)
$A_T$	Total alkalinity	Variable	$\text{equiv dm}^{-3}$	powtra(:, :, :, ipowaal)
$\text{PO}_4$	Phosphate	Variable	$\text{mol}_P \text{ dm}^{-3}$	powtra(:, :, :, ipowaph)
$\text{O}_2$	Oxygen	Variable	$\text{mol}_{\text{O}_2} \text{ dm}^{-3}$	powtra(:, :, :, ipowaiox)
$\text{N}_2$	Molecular nitrogen	Variable	$\text{mol}_N \text{ dm}^{-3}$	powtra(:, :, :, ipown2)
$\text{NO}_3$	Nitrate	Variable	$\text{mol}_N \text{ dm}^{-3}$	powtra(:, :, :, ipowno3)
$\text{Si(OH)}_4$	Silicic acid	Variable	$\text{mol}_{Si} \text{ dm}^{-3}$	powtra(:, :, :, ipowasi)
<i>parameters</i>				
$v_{s \rightarrow d}$	Dissolution reaction rate	Variable	$\text{kmol m}^{-3} \text{ s}^{-1}$	
$\rho$	Bulk sediment density	Variable	$\text{kg m}^{-3}$	sedlo
$\rho_{\text{CaCO}_3}$	Density of $\text{CaCO}_3$	2600	$\text{kg m}^{-3}$	calcdens
$\rho_{\text{bSiO}_2}$	Density of $\text{bSiO}_2$	2200	$\text{kg m}^{-3}$	opaldens
$\rho_{\text{OC}}$	Density of organic carbon	1000	$\text{kg m}^{-3}$	orgdens
$\rho_{\text{clay}}$	Density of clay (quartz)	2600	$\text{kg m}^{-3}$	claydens
$M_{\text{CaCO}_3}$	Molecular weight of $\text{CaCO}_3$	100	$\text{kg kmol}^{-1}$	calcwei
$M_{\text{bSiO}_2}$	Molecular weight of $\text{bSiO}_2$	60	$\text{kg kmol}^{-1}$	opalwei
$M_{\text{OC}}$	Molecular weight of organic carbon	100	$\text{kg kmol}^{-1}$	orgwei
$R$	Stoichiometric ratio C : P	122	–	rcar
$R$	Stoichiometric ratio N : P	16	–	rnit, rno3
$R$	Stoichiometric ratio $-\text{O}_2$ : P	172	–	ro2ut
$\mathcal{B}$	Bioturbation diffusion coefficient	$1.0 \times 10^{-9}$	$\text{m}^2 \text{ s}^{-1}$	sedict
$\mathcal{D}$	Porewater diffusion coefficient	$1.0 \times 10^{-9}$	$\text{m}^2 \text{ s}^{-1}$	sedict
$\phi$	Porosity	0.62 to 0.85	–	porwat(:)
$V_f$	Total solid sediment volume	$\approx 1 - \phi$	–	solfu

**Table A1.** The sediment model's parameters and variables with values, associated units, and variable names in the Fortran code of BLOM/iHAMOCC.

## Appendix B: Postprocessing and analysis

Here is shown how the model output is processed and analysed. Besides for reproduction of the final results, the reader may freely use any or all of these methods and code for their own purpose, though most of it is quite specific for BLOM/iHAMOCC output.

The pipelines are partial, or partially automated if you will. The scripts depend on CDO and Ferret. The relevant scripts can be accessed at <https://hg.sr.ht/~marco/sediment-analysis>. After running the model, a model output file must be given as input to `process4analysis`, and an output directory can optionally be specified as well:

```
process4analysis -i model-output.nc -o processed
```

This pipeline ends with an `out.nc` in your output directory. Go into that directory and run `plot-tracers.gnuplot`, e.g. with the `load` command on the Gnuplot prompt, to make timeseries plots.

On your system you may need to remove or modify the `module load` commands. Note that `strftime(3)` as implemented in the GNU C Library can handle years beyond 9999, which may be useful for long simulations. For six digits you can use a conversion specification of `%06Y`. This is not part of BSD libc or the ISO C standard.

For maps in either the seawater or the sediment or transects, one may consider using ComPlot; full documentation is included in that package.

## Appendix C: Recommendations

The development, implementation, simulation and analysis of this burst-coupling method took a much longer time than expected. This was due to a combination of several reasons, but here the main author will give only the technical (and perhaps philosophical) elements that played a role. This could be useful for those who consider doing something similar.

The climate system is complex and it is only a wonder that we mortals are able to capture some of its complexity in a quantitative simulation model. As a consequence, climate models are bound to be complex as well; otherwise they would not be a good representation of reality. Of course, they do not need to be close to a complete representation of reality, because models of low complexity that describe only one or a small subset of mechanisms can be very useful to investigate those mechanisms. However, here I talk about models of high complexity that are created to be used for prognostic purposes (e.g. CMIP projections).

The model that is used in this study is BLOM/iHAMOCC, which is part of NorESM. BLOM/iHAMOCC is developed to be used as part of CMIP projections and it is always the question, and it should be considered, if one should use it for other studies as well.<sup>2</sup> In the case of this study this is probably warranted, because of the opportunity to run the model efficiently to a steady state, which is a useful starting point for almost any simulation including for the CMIP. The sediment component of the model is in fact suitable for the long-term simulations, because it is fast whilst still of sufficient complexity for the purposes here.

That said, the motivation to use this model is politically driven. Every nation state that feels important must run their own model, or so the emergent driving power of the descientised enterprise thinks. This is a waste of resources, both computational and people-wise. It is better to choose a model or method based on more scientific grounds.

Again, the way BLOM/iHAMOCC has been used in this study is not particularly bad. However, its coding quality is not very high. It is at least behind at least some other models. One example is NEMO.<sup>3</sup> This statement is of course not consistent with *model democracy*, something that is often presumed but never really tested. Of course there are model intercomparison studies and the models get evaluated (visually, goodness-of-fit and so), which shows that some models are much better than others, but the idea of model democracy persists.

Besides the usual way of evaluating through one or more goodness-of-fits, another notion of reliability is generally ignored throughout the literature (e.g. Hulten, M.M.P. van, 2014, §2.4). In this second sense, NorESM and at least some of its components, notably BLOM/iHAMOCC, are not reliable. This becomes clear from even superficial code and code structure inspection. Both the efforts that came from this study as well as more recent developments (Tjiputra et al., 2020) have improved this a lot, but there is still a lot to be desired. In this sense it will always be behind certain other models like NEMO. There are good reasons for this. The modelling team of the “French” model NEMO (and the larger IPSL model and even the PISCES biogeochemical subcomponent of NEMO) is larger. This should be taken at face value and as such the choice of using BLOM/iHAMOCC was possibly the wrong one.

That said, NEMO does not have a proper sediment component (there is something but it is not recently tested or well developed). That is a motivation to use another model or implement a sediment model. Nonetheless, it is not sufficient reason to use BLOM/iHAMOCC for this.

One of the difficulties with implementing the burst-coupling method into BLOM/iHAMOCC was that the code was not well written. It had little consistency and its structure is hard to follow. After the main author had refactored and debugged a part of the code, the model ran about 20 % faster in coupled mode. Some guidelines were adopted and used throughout the model code. This can be seen by browsing through the commits of the last year or the last couple of years. The way of developing the model as a community has improved as well. This is largely due to its availability through a public repository and that it is published under a free software license. At the same time, culture change is slow and a stronger DevOps philosophy could strengthen the model’s development further. The recent coding efforts made the code undoubtedly more readable, less buggy and more efficient. In the meantime, other models have improved as well. Whether to continue using NorESM for CMIP simulations, and whether to use this model and BLOM/iHAMOCC for a specific study, should be carefully considered and also evaluated during development.

If it is decided to use NorESM and BLOM/iHAMOCC for further studies, I would recommend introducing the latest and best version of the burst-coupling code in a more current, stable version of NorESM. The long burst simulation should then be repeated and an evaluation of the sediment and reevaluation of the seawater should be performed.

<sup>2</sup>There is also a discussion if and in what way the many model simulations as part of CMIP are useful, but the answer to that is far from trivial and I will not discuss that here.

<sup>3</sup>The main author is familiar only with the intrinsics of NEMO and BLOM/iHAMOCC, but all statements made in these recommendations can be made based on only those two.